MOLECULAR AND CELLULAR BIOLOGY, Dec. 2011, p. 4917–4927 Vol. 31, No. 24
0270-7306/11/$12.00 doi:10.1128/MCB.05799-11

PHLPP-Mediated Dephosphorylation of S6K1 Inhibits Protein Translation and Cell Growth▽

Jianyu Liu,[1] Payton D. Stevens,[1] Xin Li,[1] Micheal D. Schmidt,[1] and Tianyan Gao[1,2]*

Markey Cancer Center[1] and Department of Molecular and Cellular Biochemistry,[2] University of Kentucky, Lexington, Kentucky 40536-0509

Received 13 June 2011/Returned for modification 22 July 2011/Accepted 3 October 2011

PHLPP is a family of Ser/Thr protein phosphatases that contains PHLPP1 and PHLPP2 isoforms. We have shown previously that PHLPP functions as a tumor suppressor by negatively regulating Akt signaling in cancer cells. Here we report the identification of ribosomal protein S6 kinase 1 (S6K1) as a novel substrate of PHLPP. Overexpression of both PHLPP isoforms resulted in a decrease in S6K1 phosphorylation in cells, and this PHLPP-mediated dephosphorylation of S6K1 was independent of its ability to dephosphorylate Akt. Conversely, S6K1 phosphorylation was increased in cells depleted of PHLPP expression. Furthermore, we showed that the insulin receptor substrate 1 (IRS-1) expression and insulin-induced Akt phosphorylation were significantly decreased as the result of activation of the S6K-dependent negative feedback loop in PHLPP knockdown cells. Functionally, the phosphorylation of ribosomal protein S6 (rpS6) and the amount of phosphorylated rpS6 bound to the translation initiation complex were increased in PHLPP-knockdown cells. This correlated with increased cell size, protein content, and rate of cap-dependent translation. Taken together, our results demonstrate that loss of PHLPP expression activates the S6K-dependent negative feedback loop and that PHLPP is a novel player involved in regulating protein translation initiation and cell size via direct dephosphorylation of S6K1.

Precise control of cell signaling is achieved by balancing a vast pool of protein phosphorylation events with a limited number of protein phosphatases. The involvement of protein phosphatases in regulating many fundamentally important cellular processes has been appreciated only recently (32). PHLPP represents a novel family of Ser/Thr protein phosphatases. Two isoforms of PHLPP, namely, PHLPP1 and PHLPP2, sharing ~50% identity at the amino acid level, are found in this phosphatase family (3, 8). To date, members of the AGC kinase superfamily, including Akt and conventional protein kinase C (PKC) isozymes, have been identified as substrates of PHLPP. Both Akt and PKC are known to be regulated by protein phosphorylation, and PHLPP-mediated dephosphorylation leads to inactivation or accelerated degradation (2). In the case of Akt, our previous studies demonstrate that PHLPP-mediated dephosphorylation of Akt results in an increase in apoptosis and a decrease in cell proliferation, and loss of PHLPP expression occurs with high frequency in colorectal cancers (3, 8, 16). In the case of PKC, the cellular expression level of conventional PKC isozymes is negatively regulated by PHLPP, as PHLPP-mediated dephosphorylation leads to degradation of PKC (7). Intriguingly, PHLPP preferentially dephosphorylates the hydrophobic motif of both Akt and PKC, demonstrating a unique specificity not commonly observed in Ser/Thr protein phosphatases (2). Given the fact that the hydrophobic motif phosphorylation site is highly conserved within members of the AGC kinase superfamily, it is of particular interest to investigate whether other kinases in this family are also substrates of PHLPP.

S6K1 (also named p70 S6K) is a closely related cousin of Akt and PKC in the AGC kinase family. Activation of S6K1 is controlled by signaling inputs from growth factor, nutrient, and energy balance directly downstream of mTOR. Like Akt, full and sustained activation of S6K1 requires phosphorylation at two essential sites: the activation loop (T229) and the hydrophobic motif (T389). Specifically, in response to growth factor stimulation, S6K1 is phosphorylated by mTOR in the rapamycin-sensitive complex (TORC1) at T389 and subsequently phosphorylated at T229 by PDK-1 (21). In addition, S6K activity is also tightly regulated by amino acid availability downstream of mTOR. Amino acid deprivation effectively turns off the mTOR activity, leading to decreased phosphorylation of S6K and a dramatic reduction of protein translation (25, 26).

As S6K1 serves as one of the major substrates of mTOR, activation of S6K1 positively regulates protein translation by phosphorylating several components required for translation initiation (17). S6K1 itself when in its inactivated state is associated with eukaryotic initiation factor 3 (eIF3) in the translation initiation complex and rapidly released upon phosphorylation by mTOR. This dissociation of S6K1 allows it to be activated by PDK-1, leading to phosphorylation of its substrate eIF4B (11). Genetic studies have revealed that S6K1 plays an important role in controlling cell size (20). S6K1-knockout mice are significantly smaller due to a decrease in the size of all organs (29). Similarly, mouse embryonic fibroblast (MEF) cells derived from knock-in mice carrying a phosphorylation-deficient mutant ribosomal protein S6 (rpS6) allele (in which all five S6K phosphorylation sites in rpS6 are replaced with alanines) are significantly smaller (24). Thus, S6K1 and its substrate rpS6 are directly involved in determining cell size.

* Corresponding author. Mailing address: Department of Molecular and Cellular Biochemistry, University of Kentucky, Lexington, KY 40536-0509. Phone: (859) 323-3454. Fax: (859) 323-2074. E-mail: tianyan.gao@uky.edu.

▽ Published ahead of print on 10 October 2011.

Although S6K is activated downstream of the phosphatidylinositol 3-kinase (PI3K)/Akt pathway, many recent studies have demonstrated that activation of S6K triggers a negative feedback regulation of the pathway via downregulation of IRS-1 (18). The existence of the negative feedback loop has been exemplified by the loss-of-function mutations found in TSC2 gene-associated tuberous sclerosis and other hamartoma syndromes (12). Hyperactivation of mTOR and S6K1 as the result of decreased TSC2 function leads to S6K-mediated phosphorylation and degradation of IRS-1 protein. Subsequently, activation of Akt downstream of insulin or insulin-like growth factor 1 (IGF-1) receptors is strongly suppressed (10, 18). Moreover, the negative regulation imposed upon PI3K signaling by TSC2 mutations can be released by treating cells with rapamycin (18).

In this study, we report the identification of S6K1 as a substrate of PHLPP. We show that the hydrophobic motif of S6K1 is specifically dephosphorylated by PHLPP *in vitro* and in cells. In addition, we examine the contribution of PHLPP in regulating the S6K-dependent negative feedback loop.

MATERIALS AND METHODS

Reagents and antibodies. The expression plasmids for hemagglutinin (HA)-tagged S6K1, glutathione *S*-transferase (GST)-tagged S6 (substrate of S6K), and a dual-*Renilla*-firefly-luciferase pcDNA3-rLuc-PolioIRES-fLuc reporter were generously provided by John Blenis (Harvard Medical School). The following antibodies were purchased from commercial sources: polyclonal antibodies for PHLPP1 and PHLPP2 from Bethyl Laboratory; polyclonal antibodies against Akt, 4E-BP1, S6K1, eIF4E, mTOR, rpS6, phospho-Akt (pT308 and pS473), phospho-S6K1 (pT389), phospho-rpS6 (pS235/236), phospho-PRAS40 (pT246), phospho-4E-BP1 (pT37/46), and phospho-mTOR (pS2448) from Cell Signaling; mouse monoclonal antibody (MAb) against S6K1 and goat polyclonal antibody against eIF4b from Santa Cruz; phospho-p70S6K (pT229) from R&D Systems; and anti-γ-tubulin MAb from Sigma. 7-Methyl-GTP Sepharose 4B (m^7GTP beads) and PreScission protease were obtained from GE Healthcare. Anti-HA affinity matrix of rat IgG1 was purchased from Roche Applied Science.

Cells. Human colon cancer cell lines HT29 and KM20 were cultured in McCoy's 5A and minimal essential medium (MEM) (supplemented with 1 mM sodium pyruvate, 0.1 mM nonessential amino acids, and 2× vitamin solution), respectively. 293E and mouse embryonic fibroblast (MEF) cells were cultured in Dulbecco modified Eagle medium (DMEM). All media were supplemented with 10% fetal bovine serum (FBS; HyClone) and penicillin-streptomycin. The short hairpin RNAs (shRNAs) for human PHLPP1, PHLPP2, and PPP2CA (targeting sequence 5′-ACTATTGTTATCGTTGTGGTA-3′) were constructed in the pLKO.1-puro vector, and the lentivirus-mediated delivery of shRNA and selection for stable knockdown cells were carried out as previously described (16). The stable cells overexpressing HA-PHLPP1 or HA-PHLPP2 were generated by infecting cells with retrovirus encoding each PHLPP isoform and selected against puromycin (16). The cell size was measured using a Beckman Coulter Vi-Cell cell viability analyzer.

Isolation and immortalization of PHLPP1$^{-/-}$ mouse embryonic fibroblast (MEF) cells. The PHLPP1-knockout (PHLPP1$^{-/-}$) mice were kindly provided by A. Newton (19). The wild-type (WT) and PHLPP1$^{-/-}$ mice used for breeding were littermates in a B6/129 mixed background. The MEF cells were isolated from wild-type and PHLPP1$^{-/-}$ mouse embryos at day 14 of gestation by following standard protocols (33). The primary MEF cells were immortalized using lentivirus-mediated knockdown of p53 using pLKO.1-puro-shp53 (Addgene).

IP and immunoblotting. The detergent-solubilized cell lysates were obtained after lysing cells in lysis buffer (50 mM Na_2HPO_4, 1 mM sodium pyrophosphate, 20 mM NaF, 2 mM EDTA, 2 mM EGTA, 1% Triton X-100, 1 mM dithiothreitol [DTT], 200 μM benzamidine, 40 μg ml^{-1} leupeptin, 200 μM phenylmethylsulfonyl fluoride [PMSF]) (8). For immunoblotting analysis, the same amount of cell lysates was directly separated by SDS-PAGE. Immunoprecipitation (IP) experiments were performed according to procedures described previously (14). For cap binding assays, cell lysates were incubated with 7-methyl-GTP (m^7GTP) Sepharose at 4°C for 2 h as described previously (11). Immunoprecipitates were washed with lysis buffer, and bound proteins were analyzed by SDS-PAGE and immunoblotting. The density of Western blot signals was obtained and quantified using a FluoChem digital imaging system (Alpha Innotech).

***In vitro* dephosphorylation.** The PP2C domain of PHLPP1 or PHLPP2 was cloned into the pGEX-6P-3 vector, and GST-tagged P1-PP2C and P2-PP2C fusion proteins were expressed and purified from bacteria as described previously (3, 8). The GST-PP2C was treated with PreScission protease to release PP2C recombinant proteins. To obtain phosphorylated p70S6K proteins as substrate, 293T cells transfected with HA-S6K1 were lysed in lysis buffer. Cell lysates were incubated with anti-HA affinity matrix, and the immunoprecipitates were washed twice with lysis buffer and twice with phosphatase buffer (0.1 M sodium acetate, 0.05 M bis-Tris, 0.05 M Tris, pH 7.5). The dephosphorylation reactions were carried out by incubating HA-S6K1-bound beads with purified P1-PP2C or P1-PP2C (0.1 μg) at room temperature for 0 to 30 min in the phosphatase buffer supplemented with $MnCl_2$ (2 mM) and DTT (10 mM) (8). For subsequent kinase assays following dephosphorylation, HA-S6K1-bound beads were treated with P1-PP2C for 30 min and washed twice in lysis buffer and twice in kinase buffer (25 mM Tris-HCl, pH 7.4, 10 mM $MgCl_2$, 5 mM β-glycerophosphate). The purified GST-S6 (1 μg per reaction mixture) and ATP (200 μM) were added to the HA-S6K1 beads to initiate the phosphorylation (23). The kinase reactions were carried out at 30°C for 30 min.

Amino acid starvation and stimulation of cells. For amino acid starvation, cells grown in serum-containing medium were rinsed with and incubated in amino acid-free and serum-free MEM (supplemented with 584 μg/ml L-glutamine) for 50 min. Subsequently, cells were stimulated by switching to regular serum-free DMEM containing a normal concentration of amino acids for 1 h (15). Cell lysates were prepared in lysis buffer and subjected to immunoprecipitation and immunoblotting analysis.

Dual-luciferase assay. A dual-luciferase reporter with the hypoxia-inducible factor 1α (HIF-1α) 5′ untranslated region (UTR) inserted in front of the *Renilla* luciferase and the poliovirus internal ribosome entry site (IRES) driving the firefly luciferase was used to determine the cap-dependent translation (4). Cells transfected with the dual-luciferase reporter were treated as specified, and the luciferase activities were measured using a dual-luciferase reporter assay system (Promega). The cap-dependent translation was defined as the ratio of *Renilla* to firefly luciferase activities.

RESULTS

Phosphorylation of S6K1 is regulated by PHLPP. In our experiments examining the effect of PHLPP on Akt phosphorylation, we observed that the phosphorylation of endogenous Akt at S473 was decreased in stable PHLPP1- or PHLPP2-overexpressing colon cancer or 293E cells, consistent with our previous findings in other cell lines (Fig. 1A) (3, 8, 16). Given the notion that S6K1 is regulated downstream of Akt, the phosphorylation of S6K1 at T389 was also decreased in cells overexpressing either PHLPP isoform (Fig. 1A). The extents of PHLPP-induced dephosphorylation of Akt and S6K1 were similar in all cell lines examined (Fig. 1B). However, to our surprise, knockdown of each PHLPP isoform resulted in an increase in S6K1 phosphorylation at both T229 and T389 sites but a decrease in Akt phosphorylation at both T308 and S473 sites (Fig. 2A and B). In addition, the activity of S6K1 was also increased as indicated by elevated phosphorylation of its downstream substrate rpS6 (Fig. 2A). Since this paradoxical uncoupling of Akt and S6K1 phosphorylation was also seen in TSC2-knockdown cells in which the negative feedback loop is activated (18), we hypothesized that knockdown of PHLPP directly activates S6K1 and triggers the negative feedback regulation of Akt in these cells. In addition, knockdown of both PHLPP isoforms further increased the phosphorylation of S6K1 at both phosphorylation sites by ~2-fold (Fig. 2C), suggesting that the two PHLPP isoforms function nonredundantly in suppressing S6K1 phosphorylation. However, knockdown of a single PHLPP isoform was sufficient to fully activate the negative feedback regulation of Akt, as the extents of Akt

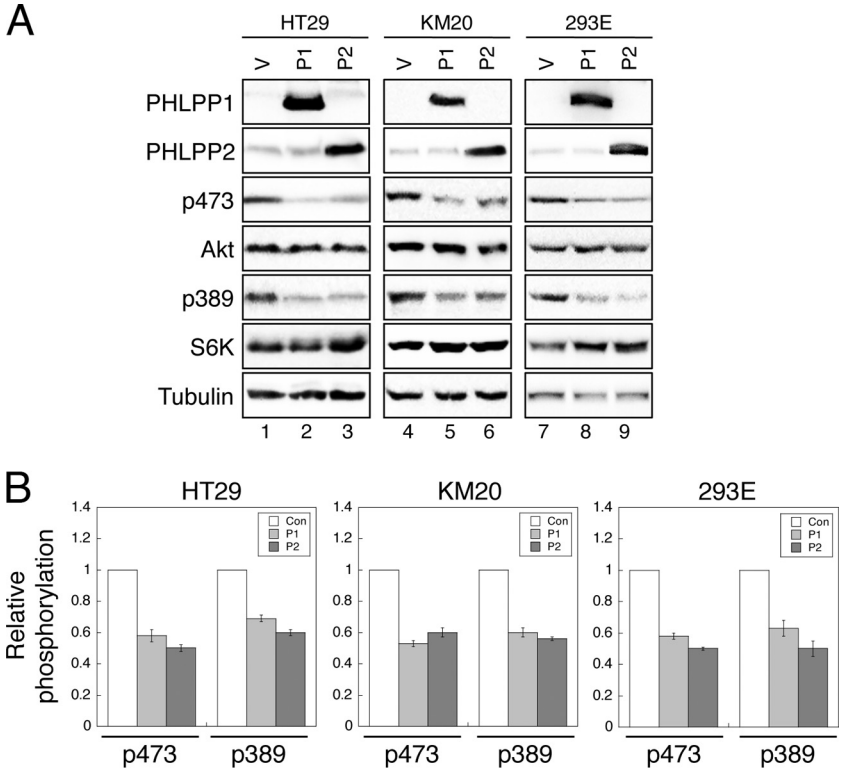

FIG. 1. Overexpression of PHLPP results in dephosphorylation of both Akt and p70S6K. (A) Dephosphorylation of Akt and S6K1 was analyzed in stable HT29 (lanes 1 to 3), KM20 (lanes 4 to 6), and 293E (lanes 7 to 9) cells overexpressing PHLPP1 or PHLPP2. The phosphorylation status of Akt at S473 and that of p70S6K at T389 in cell lysates were detected using the phospho-S473 (p473) and phospho-T389 (p389) antibodies, respectively. (B) Western blotting results as shown in panel A were quantified using the FluoChem digital imaging system. The relative phosphorylation of Akt and S6K1 was quantified by normalizing enhanced chemiluminescence signals generated by the phospho-specific antibodies to that of total Akt or S6K1 proteins, and the quantitative results were expressed graphically. Data shown in the graph represent the means ± standard errors of the means ($n = 3$).

inhibition were similar in cells with single and those with double knockdown of PHLPP expression (Fig. 2C).

It has been reported previously that *Drosophila melanogaster* dS6K is a substrate of PP2A (1, 9). To compare PHLPP- and PP2A-mediated dephosphorylations of S6K1 in mammalian cells, we generated stable PPP2CA (formerly called PP2A catalytic subunit α isoform)-knockdown 293E cells. Interestingly, although the phosphorylation of both T229 and T389 sites in S6K1 was increased in PPP2CA-knockdown cells, PPP2CA seemed to preferentially regulate the T229 site (Fig. 2D). Moreover, only the T308 site in Akt was upregulated, whereas the phosphorylation at S473 remained unchanged in PPP2CA-knockdown cells (Fig. 2D). This finding was consistent with our previous report that the T308 and S473 sites in Akt are regulated by okadaic acid-sensitive (e.g., PP2A) and -insensitive (e.g., PHLPP) protein phosphatases, respectively (8). More importantly, only PHLPP knockdown was able to activate the negative feedback loop in cells (Fig. 2D). This is likely due to the unique substrate specificity of PHLPP in that it lacks the ability to regulate the T308 site.

Knockdown of PHLPP promotes the negative feedback regulation of the PI3K/Akt pathway via activating S6K1. To further assess whether the decrease of Akt phosphorylation observed in PHLPP knockdown cells was due to the induction of the negative feedback loop, we examined the expression level of IRS-1. Indeed, knockdown of either PHLPP isoform resulted in a marked decrease in IRS-1 expression in colon cancer HT29 and KM20 cells and 293E cells (Fig. 3A). This is consistent with previous reports that elevated activation of S6K leads to downregulation of IRS-1 proteins (10). Consequently, the phosphorylation of Akt at T308, the site controlled directly by PI3K activation, was reduced (Fig. 2A). This decrease of Akt phosphorylation at both T308 and S473 sites correlated with decreased Akt activity as indicated by reduced phosphorylation of Akt substrate PRAS40 in PHLPP-knockdown cells (Fig. 3A). Interestingly, the phosphorylation of mTOR at its autophosphorylation site was decreased in PHLPP-knockdown cells as well, suggesting decreased mTOR activity. This is further demonstrated by decreased phosphorylation of mTOR substrate 4E-BP1 (Fig. 3A).

Since Akt has previously been identified as a substrate of PHLPP (8), we postulated that PHLPP-mediated regulation of Akt was masked in these cells by the negative feedback control. As treating cells with rapamycin releases Akt from the negative feedback regulation (10), we next examined how knockdown of PHLPP affects the rapamycin-induced recovery of Akt phosphorylation. To this end, the control and PHLPP-knockdown HT29 cells were treated with rapamycin for 8 or 12 h and the phosphorylation status of Akt and S6K1 was monitored. In untreated cells, the phosphorylation of S6K1 was increased

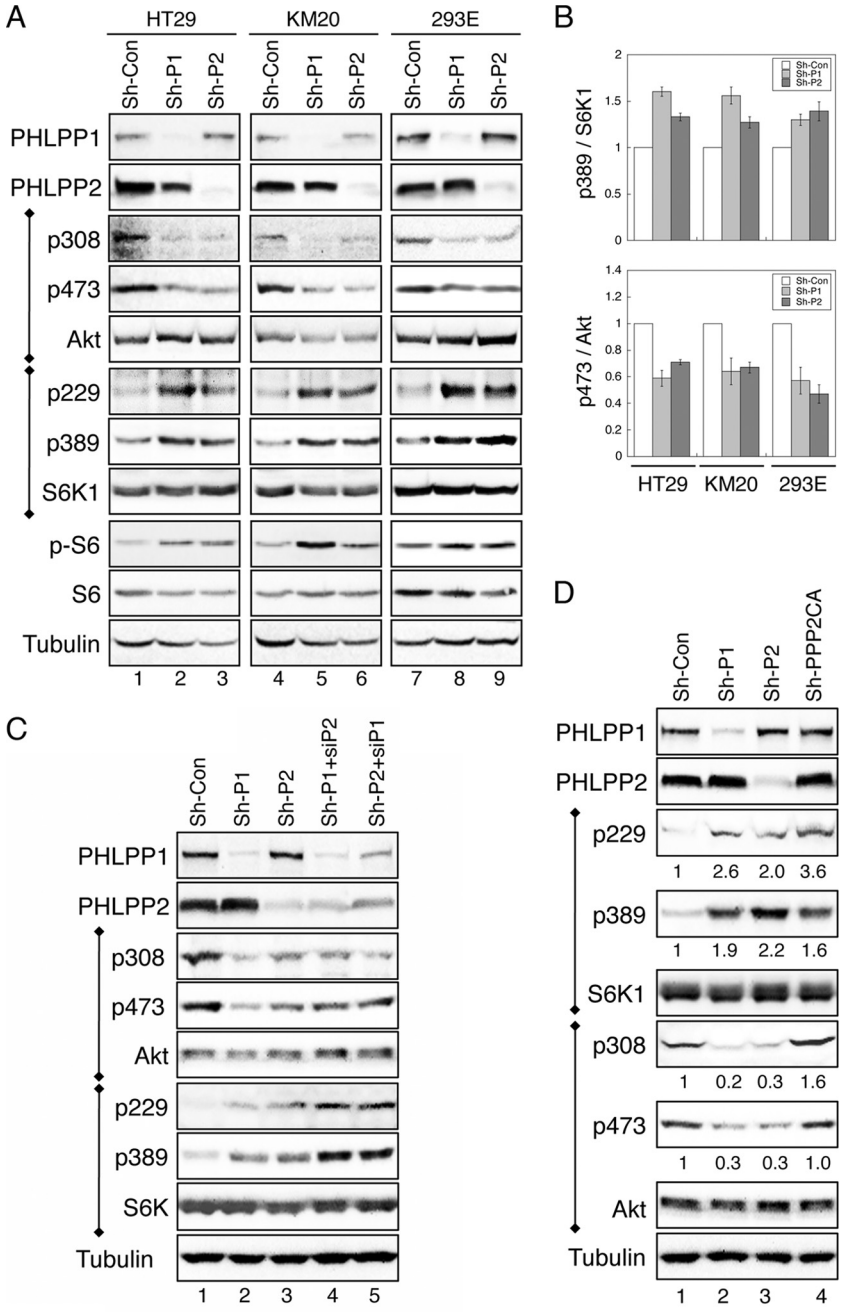

FIG. 2. PHLPP dephosphorylates S6K1 independently of Akt. (A) Knockdown of PHLPP1 or PHLPP2 resulted in an increase in S6K1 phosphorylation. Stable PHLPP1 or PHLPP2 knockdown cells were generated in HT29 (lanes 1 to 3), KM20 (lanes 4 to 6), and 293E (lanes 7 to 9) using lentivirus-mediated shRNA. The cell lysates were analyzed for the phosphorylation of Akt, S6K1, and rpS6 using phospho-specific antibodies. (B) Western blotting results as shown in panel A were quantified using the FluoChem digital imaging system. The relative phosphorylation of Akt and S6K1 was quantified by normalizing enhanced chemiluminescence signals generated by the phospho-specific antibodies to that of total Akt or S6K1 proteins, and the quantitative results were expressed graphically. Data shown in the graph represent the means ± standard errors of the means ($n = 3$). (C) The stable sh-P1 and sh-P2 293E cells were transiently infected with shRNA lentivirus targeting PHLPP2 and PHLPP1, respectively. The sh-Con, sh-P1, and sh-P2 cells were infected with control virus. Cell lysates were prepared 36 h postinfection and analyzed using Western blotting. (D) Stable sh-Con, sh-P1, sh-P2, and sh-PPP2CA 293E cells were analyzed for the phosphorylation status of S6K1 and Akt. The relative phosphorylation was quantified by normalizing enhanced chemiluminescence signals generated by the phospho-specific antibody to that of total protein and shown below the phosphoblots.

while Akt phosphorylation was decreased (Fig. 3B; also seen in Fig. 2). Rapamycin treatment resulted in a complete dephosphorylation of S6K1 (Fig. 3B). Consistent with release of the negative feedback control, the phosphorylation of Akt was increased in control cells after treatment with rapamycin for 8 h. This increase of Akt phosphorylation was further potentiated in PHLPP-knockdown cells (Fig. 3B). Moreover, while the phosphorylation of Akt started to decrease in control cells

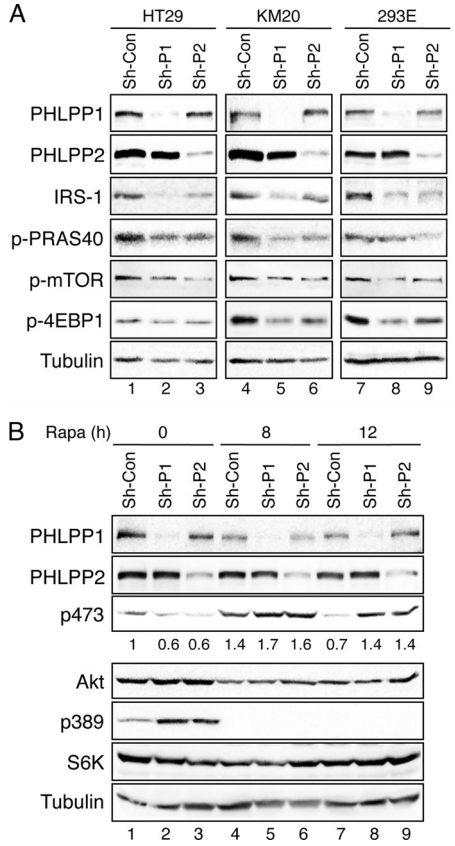

FIG. 3. Knockdown of PHLPP activates the negative feedback regulation of PI3K/Akt signaling. (A) Cell lysates prepared from stable control and PHLPP-knockdown cells, including HT29 (lanes 1 to 3), KM20 (lanes 4 to 6), and 293E (lanes 7 to 9) were analyzed for the total expression of IRS-1 and the phosphorylation status of Akt (Thr308), PRAS40 (Thr246), mTOR (Ser2481), and 4E-BP1 (Thr37/46) using Western blotting. (B) The stable control and PHLPP-knockdown HT29 cells were treated with rapamycin (20 nM) for 0, 8, and 12 h, and cell lysates were prepared and analyzed by using Western blotting. The relative phosphorylation of Akt was quantified by normalizing enhanced chemiluminescence signals generated by the p473 antibody to that of total Akt and shown below the p473 blot.

after prolonged rapamycin treatment (12 h) likely due to the disassembly of the mTORC2 complex (27), Akt remained phosphorylated in PHLPP-knockdown cells, revealing the phosphatase role of PHLPP in regulating Akt phosphorylation directly (Fig. 3B).

The involvement of PHLPP in controlling the negative feedback loop via S6K was further investigated in MEF cells derived from PHLPP1$^{-/-}$ mice (19). First, the basal level of IRS-1 was largely decreased in PHLPP1$^{-/-}$ MEF cells, and the expression started to increase after only 1 h of rapamycin treatment (Fig. 4A). After treating cells with rapamycin for 24 h, the expression of IRS-1 in PHLPP1$^{-/-}$ cells was indistinguishable from that of the wild-type (WT) cells (Fig. 4A and B). This recovery of IRS-1 expression upon rapamycin treatment is similar to what has been reported in TSC2-knockout MEF cells (10), suggesting that the S6K1-dependent negative feedback loop is activated in PHLPP1$^{-/-}$ cells. Next, the phosphorylation of Akt and S6K1 in insulin-stimulated cells was compared to that in epidermal growth factor (EGF)-stimulated cells. Since EGF receptor-mediated activation of PI3K is independent of IRS-1 (10), the phosphorylations of Akt at T308 were similar in WT and PHLPP1$^{-/-}$ cells upon EGF treatment. However, the phosphorylation of Akt at S473 was elevated in PHLPP1$^{-/-}$ cells in EGF-treated cells, consistent with the finding that PHLPP preferentially dephosphorylates the S473 site of Akt (8). In contrast, the insulin-stimulated phosphorylation of Akt at both phosphorylation sites was markedly reduced in PHLPP1$^{-/-}$ cells, and this was coincident with increased phosphorylation of S6K1. Furthermore, pretreating cells with rapamycin restored the level of Akt phosphorylation induced by insulin in PHLPP1$^{-/-}$ cells (Fig. 4C and D). Taken together, these results suggest that loss of PHLPP expression activates S6K1 and subsequently induces the negative feedback regulation of Akt. The PHLPP-mediated direct regulation of Akt can be unveiled once the negative feedback loop is blocked.

S6K1 is a direct substrate of PHLPP. Since PHLPP is known to interact with its substrates (3, 7, 8), we examined whether PHLPP and S6K1 are associated in cells. Indeed, coimmunoprecipitation of endogenous PHLPP1 or PHLPP2 with S6K1 was readily detected in HT29 and 293E cells (Fig. 5A). To further assess the PHLPP-mediated dephosphorylation of S6K1 directly, we performed *in vitro* dephosphorylation experiments using purified PP2C domains of PHLPP1 (P1-PP2C). Incubating phosphorylated S6K1 isolated from transfected 293E cells with P1-PP2C resulted in an 85% and 60% decrease in T389 and T229 phosphorylation, respectively (Fig. 5B). Once dephosphorylated by PHLPP, the kinase activity of S6K1 toward its substrate, purified GST-S6, was largely diminished (Fig. 5B). Similarly, the phosphorylation of S6K1 at both sites was dephosphorylated upon treatment with the PP2C domain of PHLPP2 but, however, to a lesser extent (data not shown). This difference in phosphatase activity was observed only *in vitro*, as the two PHLPP isoforms functioned similarly against S6K1 when overexpressed in cells (Fig. 1). Furthermore, the time course of S6K1 dephosphorylation revealed that the T389 site was rapidly dephosphorylated by P1-PP2C, and more than 80% of S6K1 became dephosphorylated within 10 min (Fig. 5C and D). In contrast, the T229 site was much less sensitive to P1-PP2C. The time needed to dephosphorylate 50% of S6K1 at T229 was 20 min compared to 5 min for T389 (Fig. 5C and D). Thus, PHLPP has a higher specificity against the T389 site of S6K1 *in vitro*. Interestingly, it has been shown previously that PHLPP is capable of preferentially dephosphorylating the hydrophobic motif sites of other substrates, including Akt and PKCβII as well (3, 7, 8). However, since the phosphorylation of S6K1 at the T389 site is absolutely required for the subsequent phosphorylation of T229 (21), it is not surprising that both sites were affected in PHLPP-knockdown cells (Fig. 2).

Since S6K1 becomes dephosphorylated in cells when subjected to amino acid starvation, we next determined the role of PHLPP in inactivating S6K1 under this physiological stress. WT and PHLPP1$^{-/-}$ MEF cells were cultured in amino acid-free medium for 0 to 45 min. As shown in Fig. 5E, S6K1 was completely dephosphorylated after 45 min of amino acid starvation in WT MEF cells. In marked contrast, the time course of S6K1 dephosphorylation was much slower and more than 40% of S6K1 remained phosphorylated at T389 at the end of

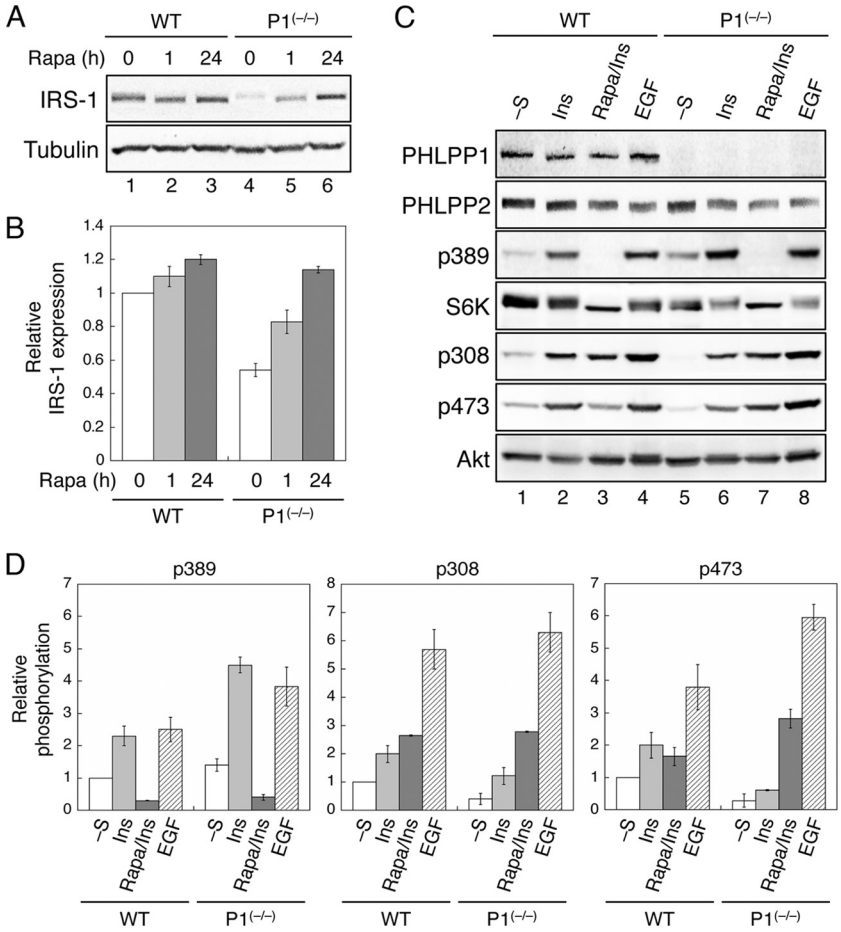

FIG. 4. Insulin-induced activation of Akt is reduced in PHLPP1-knockout MEF cells. (A) WT and PHLPP1-knockout ($P1^{-/-}$) MEF cells were treated with rapamycin (20 nM) for 0, 1, or 24 h, and the expression levels of IRS-1 were determined using the IRS-1 antibody. (B) Western blotting results as shown in panel A were quantified, and the relative expression of IRS-1 was obtained by normalizing enhanced chemiluminescence signals of IRS-1 to that of tubulin. The expression of IRS-1 in untreated WT MEF cells was set to 1, and all other conditions were normalized accordingly. Data shown in the graph represent means ± standard deviations ($n = 3$). (C) WT and $P1^{-/-}$ MEF cells were subjected to one of the following treatments: (i) serum starvation for 6 h (lanes 1 and 5), (ii) serum starvation for 6 h and subsequent stimulation with insulin (100 nM) for 10 min (lanes 2 and 6), (iii) pretreatment with rapamycin (20 nM) for 24 h and deprivation of serum during the last 6 h prior to the stimulation with insulin (100 nM) (lanes 3 and 7), and (iv) serum starvation for 6 h and subsequent stimulation with EGF (10 ng/ml) for 10 min (lanes 4 and 8). The protein and phosphoprotein levels were analyzed by Western blot analysis. (D) Western blotting results as shown in panel C were quantified using the FluoChem digital imaging system. The relative phosphorylation of Akt and S6K1 was quantified by normalizing enhanced chemiluminescence signals generated by the phospho-specific antibodies to that of total Akt or S6K1 proteins, and the quantitative results were expressed graphically. Data shown in the graph represent the means ± standard deviations ($n = 3$).

the treatment in $PHLPP1^{-/-}$ cells (Fig. 5F). The dephosphorylation of S6 followed the pattern of S6K1 and was also largely inhibited in $PHLPP1^{-/-}$ cells (Fig. 5E). Collectively, our results demonstrated that PHLPP is a key regulator of S6K dephosphorylation both *in vitro* and in cells.

PHLPP regulates S6K1 and rpS6 associated with the translation initiation complex. It has been shown previously that the level of rpS6 phosphorylation associated with the 7-methylguanosine (m^7GTP) cap complex is increased upon activation of S6K (11). In PHLPP-knockdown cells, we observed that the phosphorylation of rpS6 was increased (Fig. 2A). Here, we determined whether knockdown of PHLPP affects rpS6 associated with the cap complex. The cap structure-associated proteins were pulled down from the control and PHLPP-knockdown HT29 or 293E cells using m^7GTP beads. As shown in Fig. 6A, the phosphorylation of cap complex-bound rpS6 was increased in control cells when treated with insulin (lanes 4 and 13). This phosphorylation of rpS6 was further increased in PHLPP1- and PHLPP2-knockdown cells (lanes 5, 6, 14, and 15). Rapamycin treatment eliminated the phosphorylation of rpS6 induced by insulin (lanes 7 to 9 and 16 to 18). As a control, we showed that the amount of eIF4E, a constitutive cap-binding protein, associated with the cap complex was not altered by PHLPP expression under each treatment condition. The increase of phosphorylation in both S6K1 and rpS6 was detected in cell lysates as well (Fig. 6A). Furthermore, since the association of S6K1 with the translation preinitiation complex is inversely controlled by its phosphorylation status (11), we examined how PHLPP regulates the interaction between S6K1 and eIF3b, a critical component of the translation preinitiation complex. When grown in regular serum-containing medium, the phosphorylation of S6K1 was elevated in PHLPP-

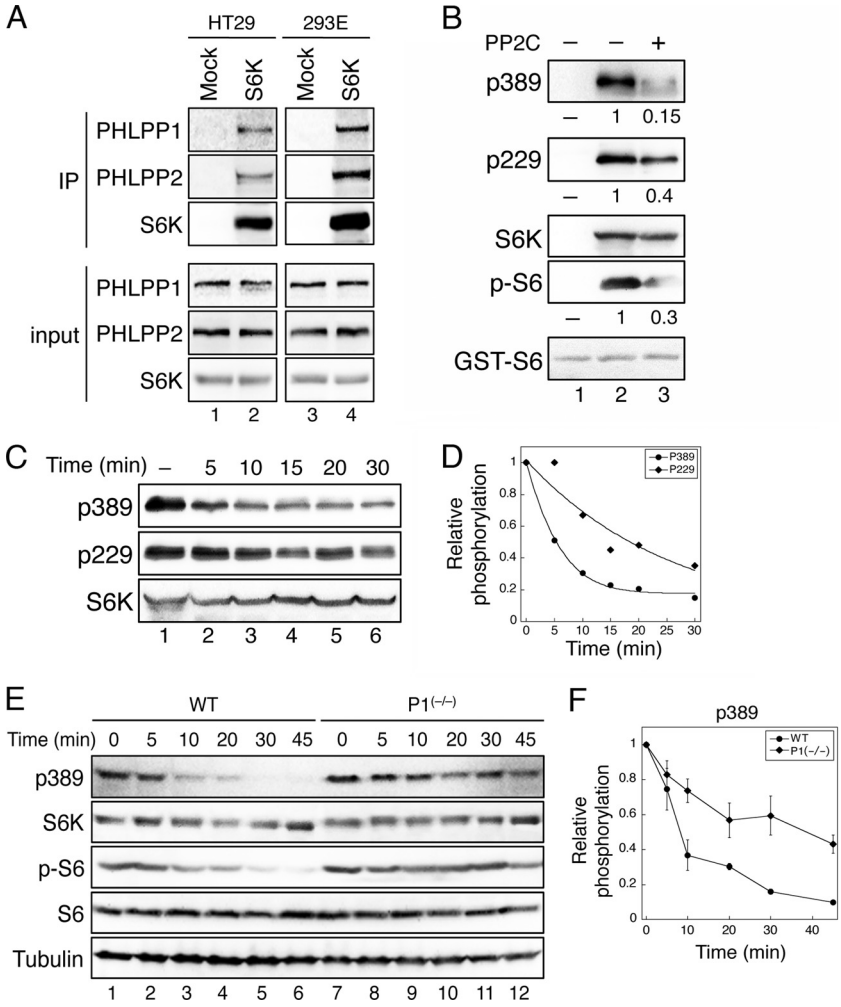

FIG. 5. S6K1 is a direct substrate of PHLPP. (A) Endogenous PHLPP and S6K1 interact. Cell lysates prepared from HT29 or 293E cells were immunoprecipitated with the anti-S6K1 antibody coupled to protein A/G beads or beads alone. The immunoprecipitates were analyzed for the presence of PHLPP1 and PHLPP2 using immunoblotting. (B) PHLPP-mediated dephosphorylation of S6K1 *in vitro*. The HA-tagged S6K1 was expressed and immunoprecipitated from 293T cells using the anti-HA affinity matrix. Dephosphorylation reactions were carried out by incubating the immunoprecipitates with the purified PP2C domain of PHLPP1 for 30 min at room temperature. The beads were then washed and incubated with purified GST-S6 in the presence of ATP. Phosphorylation of S6K1 and GST-S6 was detected using the corresponding phospho-specific antibodies. The total GST-S6 was visualized on the membrane using Ponceau S staining. The relative phosphorylation of S6K1 and GST-S6 was quantified by normalizing enhanced chemiluminescence signals generated by the phospho-specific antibodies to that of total protein and shown below the phosphoblot. (C) The time course of S6K1 dephosphorylation. The dephosphorylation reactions were carried out as described for panel B for 0 to 30 min. (D) The quantitative representation of data shown in panel C. The relative phosphorylation was quantified by normalizing enhanced chemiluminescence signals generated by the phospho-specific antibodies to that of total S6K1. The data were fitted to a single exponential curve. (E) WT and $P1^{-/-}$ MEF cells were subjected to amino acid starvation for 0 to 45 min. At each time point, the phosphorylation status of S6K1 and S6 was analyzed in cell lysates. (F) Western blotting results as shown in panel E were quantified, and the relative phosphorylation of S6K1 was quantified by normalizing enhanced chemiluminescence signals generated by p389 to that of total S6K1. Data shown in the graph represent the means ± standard deviations ($n = 3$).

knockdown HT29 cells (Fig. 6B; also shown in Fig. 2A), and this correlated with decreased binding of S6K1 with eIF3b (Fig. 6B, lanes 1 to 3). The amount of S6K1 coimmunoprecipitated with eIF3b was significantly increased as S6K1 became dephosphorylated in control cells when deprived of amino acids (Fig. 6B, lane 4). However, the binding of S6K1 with eIF3b remained low in PHLPP-knockdown cells likely due to the incomplete inactivation of S6K1 (Fig. 6B, lanes 5 and 6). Upon amino acid stimulation, S6K1 was dissociated from eIF3b as it became rephosphorylated in control cells. Knockdown of PHLPP further disrupted the interaction between S6K1 and eIF3b as the phosphorylation of S6K1 was highly potentiated (Fig. 6B, lanes 7 to 9). Similar results were obtained in the control and PHLPP-knockdown 293E cells (data not shown). Moreover, since we showed that the phosphorylation of S6K1 was more resistant to amino acid starvation in $PHLPP1^{-/-}$ MEF cells (Fig. 5E), the association of S6K1 and eIF3b remained decreased upon removal of amino acids in $PHLPP1^{-/-}$ cells compared to WT cells (Fig. 6C, lanes 1 and 2). Amino acid stimulation resulted in a larger increase in S6K phosphorylation in $PHLPP1^{-/-}$ cells and a subsequent decease in the amount of S6K binding to eIF3b compared to

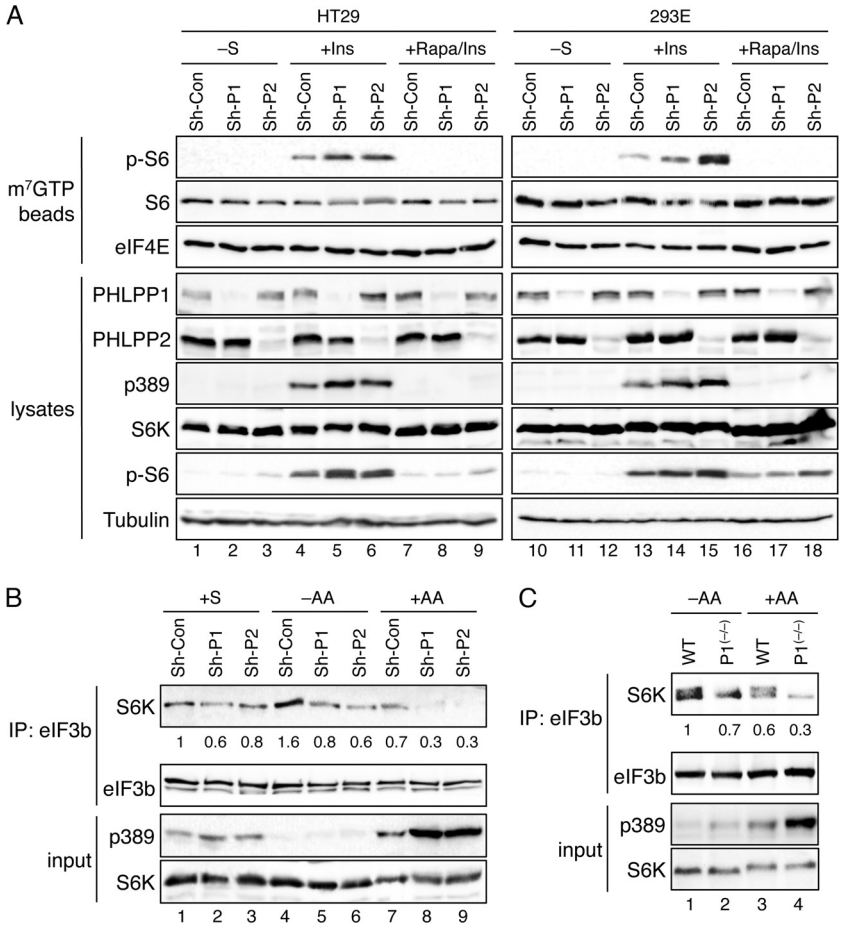

FIG. 6. PHLPP regulates the phosphorylation of rpS6 and the association of S6K1 with the translation initiation complex. (A) Knockdown of PHLPP promotes the phosphorylation of rpS6 bound with the 7-methylguanosine (m^7GTP) cap complex. The stable control and PHLPP-knockdown HT29 (lanes 1 to 9) and 293E (lanes 10 to 18) cells were serum starved overnight and subsequently treated with insulin in the presence or absence of rapamycin pretreatment. The cell lysates were incubated with m^7GTP beads to pull down cap-associated proteins. The amounts of proteins and phosphoproteins in precipitates and lysates were detected by Western blot analysis. (B) Knockdown of PHLPP decreases the binding between S6K1 and eIF3b. The stable control and PHLPP-knockdown HT29 cells grown in serum-containing medium (+S) were incubated with serum- and amino acid-free medium for 50 min (−AA) and subsequently incubated with amino acid-containing medium (+AA) for 1 h. The cell lysates were immunoprecipitated with the anti-eIF3b antibody, and the presence of S6K1 in the immunoprecipitates was determined by Western blot analysis. (C) WT and $P1^{-/-}$ MEF cells were incubated with serum- and amino acid-free medium for 50 min (−AA) and subsequently incubated with amino acid-containing medium (+AA) for 1 h. The cell lysates were immunoprecipitated with the anti-eIF3b antibody and analyzed using immunoblotting. The relative amount of S6K1 bound to eIF3b was quantified by normalizing S6K1 found in the immunoprecipitates to that in the input, and the quantitative results are shown below the S6K1 blot.

WT cells (Fig. 6C, lanes 3 and 4). Taken together, these results indicate that PHLPP plays an important role in regulating how S6K and its substrate rpS6 associate with the translation preinitiation complex and the cap structure by controlling the phosphorylation of S6K1.

PHLPP regulates cell growth and cap-dependent protein translation. It is evolutionarily conserved from *Drosophila* to human that S6K plays a positive role in maintaining cell size (20). Consistent with an inhibitory effect of PHLPP on S6K1 activity, knockdown of PHLPP1 or PHLPP2 in KM20 and 293E cells resulted in an increase in cell size and volume (Fig. 7A. In addition, $PHLPP1^{-/-}$ MEF cells were larger than the WT MEF cells (Fig. 7A). The protein content for the same numbers of cells was also significantly higher in PHLPP-knockdown cells, suggesting enhanced protein synthesis in these cells (Fig. 7B). Lastly, we examined the cap-dependent protein translation in the control and PHLPP-knockdown cells. A dual-luciferase reporter system was used to measure cap-dependent translation under different conditions. Activation of S6K1 has been shown to increase cap-dependent translation using the reporter assay (11). As shown in Fig. 7C, knockdown of either PHLPP isoform resulted in an increase in the cap-dependent translation in both KM20 and 293E cells basally. Under the serum-starved condition, the rate of cap-dependent translation was decreased as expected. However, the translation remained significantly higher in PHLPP-knockdown KM20 cells. Furthermore, insulin-stimulated translation was further enhanced by depleting PHLPP expression in both cell lines (Fig. 7C). Therefore, PHLPP plays a negative role in regulating cap-dependent translation.

In summary, our results demonstrate that the phosphorylation of S6K1 at T389 is controlled by PHLPP. Loss of PHLPP

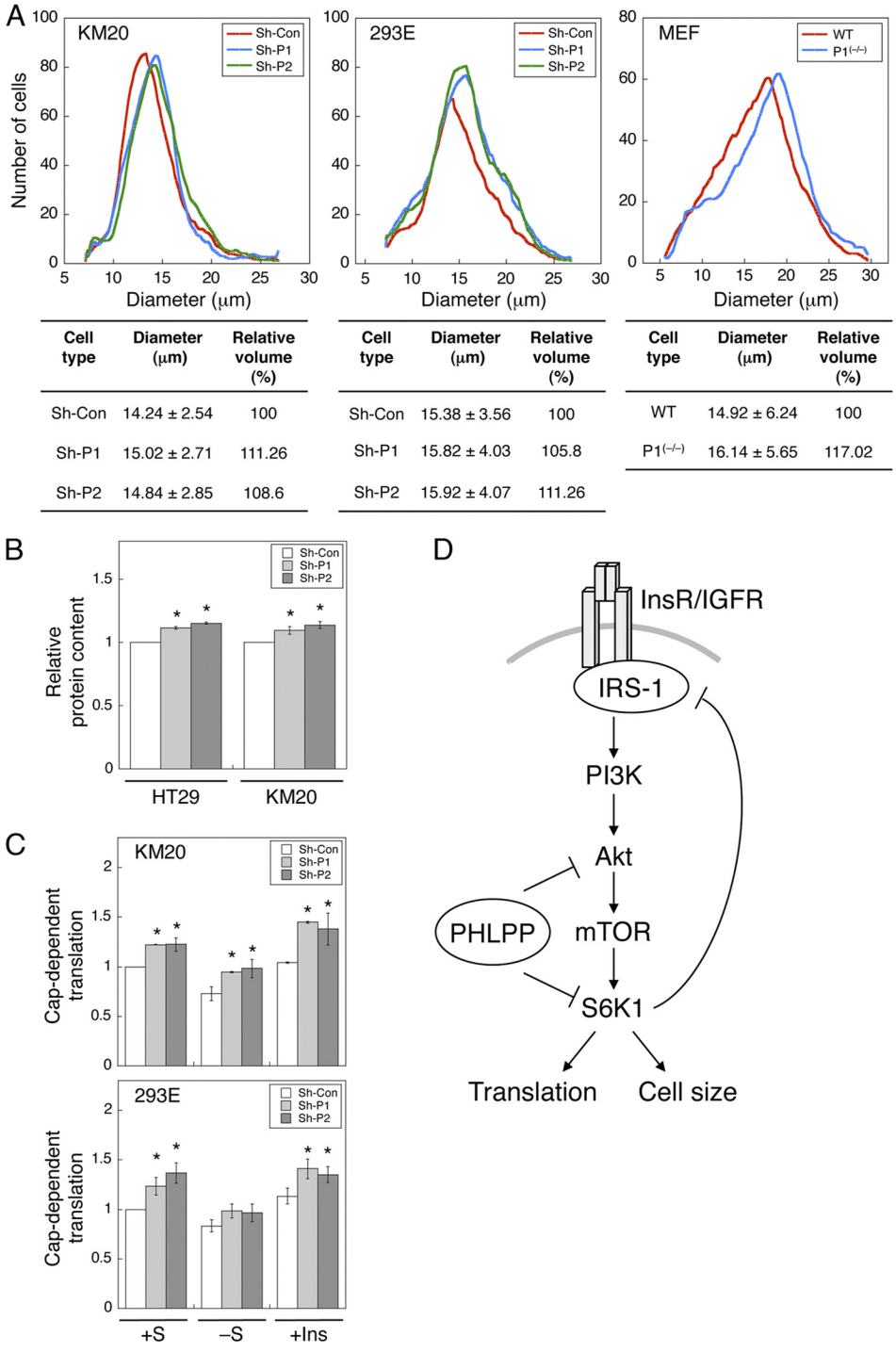

Cell type	Diameter (μm)	Relative volume (%)
Sh-Con	14.24 ± 2.54	100
Sh-P1	15.02 ± 2.71	111.26
Sh-P2	14.84 ± 2.85	108.6

Cell type	Diameter (μm)	Relative volume (%)
Sh-Con	15.38 ± 3.56	100
Sh-P1	15.82 ± 4.03	105.8
Sh-P2	15.92 ± 4.07	111.26

Cell type	Diameter (μm)	Relative volume (%)
WT	14.92 ± 6.24	100
$P1^{(-/-)}$	16.14 ± 5.65	117.02

FIG. 7. PHLPP negatively regulates cell growth and cap-dependent translation. (A) Knockdown of PHLPP increases cell size. The stable control and PHLPP-knockdown KM20 cells, 293E cells, and WT and $P1^{-/-}$ MEF cells were cultured in regular growth medium to ~50% confluence. Cell numbers were plotted against cell diameters. The average cell sizes and the relative cell volumes are shown in the tables below each graph. The cell volume was calculated based on the average diameter of each cell type. (B) Knockdown of PHLPP increases protein content in cells. Equal numbers of control and PHLPP-knockdown cells were lysed in lysis buffer, and protein concentrations were determined using Bradford assays. Each experimental point was done in duplicate, and three independent experiments were averaged and shown in the graph (mean ± standard deviation). The asterisks in all graphs indicate $P < 0.01$ as determined by two-sample t tests compared to the control cells. (C) Knockdown of PHLPP increases the cap-dependent translation. The control and PHLPP-knockdown KM20 and 293E cells were transfected with a dual-luciferase reporter. The transfected cells were subjected to one of the following treatments: (i) maintenance in serum-containing medium (+S), (ii) serum starvation overnight (−S), and (iii) serum starvation overnight followed by treatment with insulin for an additional 24 h (+Ins). Cells were collected at the same time, and luciferase activities were measured using dual-luciferase assays. The cap-dependent translation was determined using the ratio of *Renilla* to firefly luciferase light units. The value of control cells in the serum-containing medium was set to 1. Data shown in the graph represent the means ± standard deviations ($n = 3$). The asterisks in all graphs indicate $P < 0.01$ as determined by two-sample t tests compared to the control cells. (D) Diagram showing that PHLPP-mediated regulation of S6K1 alters the balance of PI3K/Akt signaling. Activation of S6K1 results in downregulation of IRS-1 expression and subsequent inhibition of Akt activity downstream of insulin/IGF-1 receptors. Our study here demonstrates that PHLPP dephosphorylates and inactivates S6K1 directly. Loss of PHLPP expression leads to activation of the S6K1-dependent negative feedback loop.

expression leads to activation of S6K1 and induction of the negative feedback loop. Thus, PHLPP negatively regulates protein translation and cell growth via controlling the S6K1 activity directly.

DISCUSSION

Hyperactivation of the PI3K/Akt/mTOR signaling pathway is one of the major driving forces in promoting tumorigenesis (6, 28). PHLPP represents a novel family of protein phosphatases that function to antagonize this pathway by dephosphorylating and inactivating Akt (3, 8, 16). In this study, we have identified S6K1 as a substrate of PHLPP both *in vitro* and in cells. Our results show that loss of PHLPP expression results in an increase in S6K1 phosphorylation and subsequent activation of the negative feedback loop. Functionally, PHLPP negatively regulates cell size and protein translation via S6K1. Taken together, our findings identify PHLPP as an integral component in the PI3K/Akt/mTOR pathway, and alteration of PHLPP expression may result in disruption of the signaling balance.

PHLPP is a phosphatase for both Akt and S6K1. We have previously shown that PHLPP preferentially dephosphorylates the hydrophobic motif of Akt and downregulates Akt signaling. Overexpression of PHLPP consistently results in a decrease in Akt phosphorylation in various cancer cells examined (3, 8, 16). It is perplexing initially that knockdown of PHLPP in a group of colon cancer cells leads to dephosphorylation of Akt as well. Our current study provides several lines of evidence indicating that S6K1 phosphorylation is directly regulated by PHLPP while the phosphorylation of Akt is indirectly controlled by the negative feedback loop: (i) PHLPP preferentially dephosphorylates S6K1 at T389 *in vitro*, (ii) dephosphorylation of S6K1 induced by amino acid starvation was slowed down significantly in PHLPP1-knockout MEF cells, and (iii) the phosphorylation of Akt is elevated in PHLPP-knockdown cells if the negative feedback loop is blocked upon rapamycin treatment. However, it is intriguing that knockdown of PHLPP in certain cell lines is directly coupled to upregulation of Akt rather than triggering the negative feedback regulation via S6K. It is possible that different pools of PHLPP that are anchored by distinct scaffolding proteins may exist in cells responsible for dephosphorylating different substrates. Further investigations are needed to determine the mechanism underlying the substrate selectivity of PHLPP in cells.

Activation of the negative feedback loop upon downregulation of PHLPP expression. In this study, we show that PHLPP shares certain similarities with TSC2 in its ability to activate the negative feedback loop. However, TSC2 mutants activate mTOR upstream of S6K, whereas loss of PHLPP expression activates S6K directly. The mTORC1 function is actually reduced in PHLPP-knockdown cells due to the inhibition of Akt activity (Fig. 3). In addition, decreased phosphorylation of PRAS40 likely contributes to downregulation of mTOR activity (31). Thus, signaling events mediated by S6K and 4E-BP1 downstream of mTOR become uncoupled in PHLPP-knockdown cells. Recent genetic studies have suggested that S6K1 plays an important role in regulating cell size whereas 4E-BPs control cell proliferation (5, 20). Consistent with these findings, both cell size and proliferation are increased in TSC2-null cells (13, 30). In contrast, the rate of proliferation is slightly decreased in PHLPP-knockdown cells used in this study (data not shown) while the cell size is increased (Fig. 7). This decrease of cell proliferation is likely due to the suppression of Akt activity and the subsequent inhibition of its downstream effectors, including mTOR. Thus, loss of PHLPP expression uniquely activates only the S6K branch of the signaling downstream of mTOR. Despite the differential outcomes of PHLPP and TSC2 downregulation, our findings here identify PHLPP as a novel component involved in the induction of the negative feedback loop.

Functional implication of PHLPP-mediated regulation of S6K1. The function of PHLPP as a tumor suppressor has been implied by a number of previous studies. Among the substrates of PHLPP, Akt and Mst1 have been shown to mediate PHLPP-dependent inhibition of cell proliferation and promotion of apoptosis (16, 22). Our findings here show that PHLPP also plays a role in controlling cell growth by regulating the activity of S6K1 directly. Although both PHLPP1 and PHLPP2 can dephosphorylate S6K1 *in vitro* and in cells, full activation of S6K1 is achieved in cells when both PHLPP isoforms are downregulated. Interestingly, loss of a single PHLPP isoform is sufficient to activate the negative feedback loop via S6K1. In addition, we show that PHLPP preferentially dephosphorylates the hydrophobic motif T389 site in S6K1 *in vitro*. However, since the phosphorylation of T389 controls the subsequent phosphorylation of T229 by PDK-1 (21), PHLPP-dependent dephosphorylation of T389 prevents the phosphorylation of T229 and the activation of S6K1 in cells. Intriguingly, the phosphatase activity of PHLPP toward S6K (and Akt) is distinct from PP2A-mediated regulation of the same substrate. Unlike PHLPP, knockdown of PP2A results in an increase in both Akt and S6K phosphorylation. We cannot rule out the possibility that PP2A regulates S6K indirectly because it also controls the activity of Akt upstream of S6K. However, our finding here that a single substrate can be dephosphorylated by multiple protein phosphatases underscores the complexity of controlling the balance of cell signaling by phosphatases. In summary, the identification of S6K1 as a novel substrate of PHLPP extends the functional role of PHLPP into regulating protein translation and cell growth. Given the growing list of cellular processes that are regulated by PHLPP, maintaining the expression of PHLPP is critical in keeping the balance of cell growth and proliferation, and loss of PHLPP expression may have multiple detrimental effects contributing to disease progression.

ACKNOWLEDGMENTS

We thank John Blenis for providing the HA-S6K1 and GST-S6 expression plasmids and 293E cells.

This work was supported by NIH R01 CA133429-01A1 (T.G.) and American Cancer Society RSG0822001TBE (T.G.).

REFERENCES

1. **Bielinski, V. A., and M. C. Mumby.** 2007. Functional analysis of the PP2A subfamily of protein phosphatases in regulating Drosophila S6 kinase. Exp. Cell Res. **313:**3117–3126.
2. **Brognard, J., and A. C. Newton.** 2008. PHLiPPing the switch on Akt and protein kinase C signaling. Trends Endocrinol. Metab. **19:**223–230.
3. **Brognard, J., E. Sierecki, T. Gao, and A. C. Newton.** 2007. PHLPP and a second isoform, PHLPP2, differentially attenuate the amplitude of Akt signaling by regulating distinct Akt isoforms. Mol. Cell **25:**917–931.
4. **Choo, A. Y., S. O. Yoon, S. G. Kim, P. P. Roux, and J. Blenis.** 2008.

Rapamycin differentially inhibits S6Ks and 4E-BP1 to mediate cell-type-specific repression of mRNA translation. Proc. Natl. Acad. Sci. U. S. A. **105:**17414–17419.
5. **Dowling, R. J., et al.** 2010. mTORC1-mediated cell proliferation, but not cell growth, controlled by the 4E-BPs. Science **328:**1172–1176.
6. **Engelman, J. A.** 2009. Targeting PI3K signalling in cancer: opportunities, challenges and limitations. Nat. Rev. Cancer **9:**550–562.
7. **Gao, T., J. Brognard, and A. C. Newton.** 2008. The phosphatase PHLPP controls the cellular levels of protein kinase C. J. Biol. Chem. **283:**6300–6311.
8. **Gao, T., F. Furnari, and A. C. Newton.** 2005. PHLPP: a phosphatase that directly dephosphorylates Akt, promotes apoptosis, and suppresses tumor growth. Mol. Cell **18:**13–24.
9. **Hahn, K., et al.** 2010. PP2A regulatory subunit PP2A-B′ counteracts S6K phosphorylation. Cell Metab. **11:**438–444.
10. **Harrington, L. S., et al.** 2004. The TSC1-2 tumor suppressor controls insulin-PI3K signaling via regulation of IRS proteins. J. Cell Biol. **166:**213–223.
11. **Holz, M. K., B. A. Ballif, S. P. Gygi, and J. Blenis.** 2005. mTOR and S6K1 mediate assembly of the translation preinitiation complex through dynamic protein interchange and ordered phosphorylation events. Cell **123:**569–580.
12. **Inoki, K., and K. L. Guan.** 2009. Tuberous sclerosis complex, implication from a rare genetic disease to common cancer treatment. Hum. Mol. Genet. **18:**R94–R100.
13. **Inoki, K., Y. Li, T. Zhu, J. Wu, and K. L. Guan.** 2002. TSC2 is phosphorylated and inhibited by Akt and suppresses mTOR signalling. Nat. Cell Biol. **4:**648–657.
14. **Li, X., J. Liu, and T. Gao.** 2009. b-TrCP-mediated ubiquitination and degradation of PHLPP1 are negatively regulated by Akt. Mol. Cell. Biol. **29:**6192–6205.
15. **Liu, J., P. D. Stevens, and T. Gao.** 2011. mTOR-dependent regulation of PHLPP expression controls the rapamycin sensitivity in cancer cells. J. Biol. Chem. **286:**6510–6520.
16. **Liu, J., et al.** 2009. Loss of PHLPP expression in colon cancer: role in proliferation and tumorigenesis. Oncogene **28:**994–1004.
17. **Ma, X. M., and J. Blenis.** 2009. Molecular mechanisms of mTOR-mediated translational control. Nat. Rev. Mol. Cell Biol. **10:**307–318.
18. **Manning, B. D.** 2004. Balancing Akt with S6K: implications for both metabolic diseases and tumorigenesis. J. Cell Biol. **167:**399–403.
19. **Masubuchi, S., et al.** 2010. Protein phosphatase PHLPP1 controls the light-induced resetting of the circadian clock. Proc. Natl. Acad. Sci. U. S. A. **107:**1642–1647.
20. **Meyuhas, O., A. Dreazen, and W. B. H. John.** 2009. Ribosomal protein S6 kinase: from TOP mRNAs to cell size. Prog. Mol. Biol. Transl. Sci. **90:**109–153.
21. **Pullen, N., et al.** 1998. Phosphorylation and activation of p70s6k by PDK1. Science **279:**707–710.
22. **Qiao, M., et al.** 2010. MstI is an interacting protein that mediates PHLPPs' induced apoptosis. Mol. Cell **38:**512–523.
23. **Roux, P. P., et al.** 2007. RAS/ERK signaling promotes site-specific ribosomal protein S6 phosphorylation via RSK and stimulates cap-dependent translation. J. Biol. Chem. **282:**14056–14064.
24. **Ruvinsky, I., et al.** 2005. Ribosomal protein S6 phosphorylation is a determinant of cell size and glucose homeostasis. Genes Dev. **19:**2199–2211.
25. **Sancak, Y., et al.** 2008. The Rag GTPases bind raptor and mediate amino acid signaling to mTORC1. Science **320:**1496–1501.
26. **Sancak, Y., and D. M. Sabatini.** 2009. Rag proteins regulate amino-acid-induced mTORC1 signalling. Biochem. Soc. Trans. **37:**289–290.
27. **Sarbassov, D. D., et al.** 2006. Prolonged rapamycin treatment inhibits mTORC2 assembly and Akt/PKB. Mol. Cell **22:**159–168.
28. **Shaw, R. J., and L. C. Cantley.** 2006. Ras, PI(3)K and mTOR signalling controls tumour cell growth. Nature **441:**424–430.
29. **Shima, H., et al.** 1998. Disruption of the p70(s6k)/p85(s6k) gene reveals a small mouse phenotype and a new functional S6 kinase. EMBO J. **17:**6649–6659.
30. **Tee, A. R., et al.** 2002. Tuberous sclerosis complex-1 and -2 gene products function together to inhibit mammalian target of rapamycin (mTOR)-mediated downstream signaling. Proc. Natl. Acad. Sci. U. S. A. **99:**13571–13576.
31. **Vander Haar, E., S. I. Lee, S. Bandhakavi, T. J. Griffin, and D. H. Kim.** 2007. Insulin signalling to mTOR mediated by the Akt/PKB substrate PRAS40. Nat. Cell Biol. **9:**316–323.
32. **Virshup, D. M., and S. Shenolikar.** 2009. From promiscuity to precision: protein phosphatases get a makeover. Mol. Cell **33:**537–545.
33. **Xu, J.** 2005. Preparation, culture, and immortalization of mouse embryonic fibroblasts. Curr. Protoc. Mol. Biol. **28:**28.1.